Divergent reward cue representations in the prefrontal cortex drive reward motivation in adolescence and adulthood

Gabriela Manzano Nieves[1], Conor Liston[1]

[1] Department of Psychiatry and Feil Family Brain and Mind Research Institute, Weill Cornell Medicine, New York, New York 10021

Keywords

Medial prefrontal cortex

Adolescence

Reward Learning

Development

Calcium Imaging

Corresponding Authors

Gabriela Manzano Nieves and Conor Liston

Emails: gmn4001@med.cornell.edu, col2004@med.cornell.edu

Abstract
Alterations in motivation and reward-seeking are a transdiagnostic feature of numerous psychiatric disorders that commonly emerge in adolescence, including depression, obsessive-compulsive disorder, and attention deficit hyperactivity disorder. During adolescence, reward motivation is naturally heightened, compared to adulthood, but the underlying mechanisms are not well understood. The medial prefrontal cortex (mPFC) is a late developing brain region that regulates reward learning and motivation and is still maturing in adolescence. The mPFC modulates reward-motivated behaviors in adults, and has been hypothesized to be responsible for adolescents' inability to suppress reward-seeking and impulsive behaviors. Using 2-photon imaging of the mPFC and an active reward task, we demonstrate that both the adult and adolescent mPFC encode reward-predictive cues, with distinct neuronal populations encoding rewarded and unrewarded cues. In adolescence the mPFC is hyper-responsive to reward cues and recruits a larger population of neurons to encode reward predictive cues. Furthermore, in the adolescent mPFC, representations of unrewarded cues are attenuated, compared to the adult mPFC, which may tip the balance of action toward reward-seeking. Differences in neuronal responses to rewarded and unrewarded cues were observed in both GABAergic and glutamatergic neurons, with GABAergic inhibition causing disparate effects in adolescents compared to adults. Together our findings identify differences in the functional properties of mPFC microcircuits in adolescents that may underlie differences in reward-seeking behavior and the ability to adaptively suppress reward seeking.

Introduction

Abnormalities in reward motivation and reward-seeking are hallmarks of various psychiatric illnesses including substance use disorder, depression, obsessive-compulsive disorder, and attention deficit hyperactivity disorder [1]. Importantly, these disorders tend to first emerge in adolescence [2]. In humans and mice, adolescence is marked by a significant increase in impulsivity, reward-seeking, and reward sensitivity compared to adulthood [3–8]. However, the neuronal representations of this increase has not been determined. Understanding how adolescents are encoding the reward information is an essential step to understand adolescent behavior, and adolescent susceptibility to the development of psychiatric disorders.

In adults, mPFC is required for learning the reward-predictive value of environmental cues, for adaptively shaping reward-seeking behavior, and for reducing impulsivity [9–12]. Infralimbic cortex of the mPFC in particular has been heavily implicated in driving reward seeking behaviors [13,14], although both prelimbic and infralimbic are known to be reward responsive [15,16]. In adolescence, brain regions and neuronal circuits that guide our ability to strategize and optimize reward outcomes are not yet fully developed. Both glutamatergic [17,18] and GABAergic neurons [19,20] are undergoing changes to their synapses, which likely results in different micro-connectivity in the adolescent mPFC, compared to the adult mPFC. Thus differences in mPFC microcircuit anatomy could be resulting in changes to the encoding properties of neurons and may lead to stereotypical "adolescent" behaviors such as increased impulsivity, reward-seeking, and reward sensitivity [3–8].

Until recently, the technical obstacles in recording neuronal activity in an animal that is still growing have made it difficult to investigate how the mPFC represents reward-motivated behavior in adolescence. To overcome these challenges, we created custom made behavioral apparatuses that can be adapted to fit juvenile, adolescent, and adult mice, to allow for recording calcium activity via an implanted optical prism [21] across development. We also created a custom behavioral protocol that allowed for fast learning of a reward-association task, allowing us to train and test mice in adolescence. We leveraged these new innovations to

assess how mPFC neurons represent reward and no-reward cues in adolescence and adulthood.

Results

An active reward task for head-fixed mice

To assess reward-motivated behaviors, we developed an active reward task compatible with head-fixed 2-photon imaging, that we first tested in adults. The active reward task permits analysis of general learning, motivational drive and inhibitory control. A trial begins with the onset of a conditioned stimulus (CS, tone, 5 second duration), mice's response (lick to spout) during this tone period is used to determine outcome (**Fig. 1A**). If the reward predicting CS (CS+) plays, mice can lick the spout (hit) to obtain a reward at tone offset, or abstain from licking the spout (miss) to forgo a reward. For the first 3 days, mice are trained to a single rewarded tone (CS+ only, **Fig. 1B**). Following CS+ only training, a CS- (not rewarded) is introduced to the task (**Fig. 1C**). If mice lick to the CS-, it is considered a false alarm; if they abstain from licking the CS-, it is considered a correct rejection. During CS+/CS- trials, mice learn to lick to the CS+, but not the CS-. Trials acquired (at least one lick during CS) and the lick rate (Hz) can be observed to change with learning in individual adult mouse data (**Fig. 1D**). Adult group data shows how the percent of acquired trials changes as a session progresses (**Fig. 1E**). In general, during CS+ only training, we find that adults have a steady increase in hit trials, although lick rate to hits does not increase (**Fig. 1F**). Once the CS- is introduced (CS+/CS-), adult mice steadily learn to stop responding to CS- trials and decrease their lick rates during false alarms. Lastly, we observe that adult lick rates to the reward (post hit trials) are significantly higher than post false alarms, where no reward is delivered (**Fig. 1G**). Together this data demonstrates that adults can learn the active reward task and can learn to distinguish CS+ and CS-.

Neuronal representation of behavioral outcomes in adults

We then used 2-photon calcium imaging to record neuronal activity of mPFC neurons as mice performed the active reward task. We conducted experiments in transgenic mice that expressed a red reporter (Ai9) in GABAergic neurons (Gad2-cre) and used a viral vector to express the calcium indicator GCaMP8f in all cells (**Fig. 2A**). This strategy allowed us to simultaneously record predominantly Glutamatergic (Ai9 negative) and GABAergic (Ai9 positive) neurons. To observe the neuronal activity related to reward and no-reward cues, we analyzed data during the seventh day of CS+/CS- conditioning, when mice are presented with 60 CS+ and 60 CS- tones, with four possible behavioral outcomes (**Fig. 2B**).

To investigate the coding properties of mPFC neurons in the context of our active reward task and identify task-relevant neurons, we used a general linear model (GLM) with three predictors (CS+, CS-, and Lick; **Fig. 2C**). Together, these predictors were utilized for neuronal classification and for comparing their activity across four potential trial outcomes (Hit, Miss, Correct Rejection, and False Alarm). Only pretone and tone data was used for the classification of neurons as task-relevant during the tone. For adults, we found that 1335 out of 2795 neurons (47.7%) were task-relevant, with 154 being identified as GABAergic (**Fig. 2D**).

To test for differences in neuronal activity for each of the four possible outcomes (hit, miss, correct rejection, and false alarm), we compared the mean z-scored tone activity (mean of 0-5s) of glutamatergic (top) and GABAergic (bottom) task-relevant neurons (**Fig. 2E**). For z-scores, the first 2.5 seconds of the pretone activity was used as the baseline activity of each trial. In adult glutamatergic neurons, we found that the mean of all task-relevant neurons was

significantly greater during correct rejections and false alarms (both CS- outcomes) compared to hit and miss outcomes (both CS+ outcomes). This finding may suggest that the adult mPFC may be more responsive to no-reward cues. In adult GABAergic neurons, no significant global differences in tone responses were observed across the 4 task outcomes.

To further explore the relationship between the calcium activity of neurons during outcomes that have the same CS but different behavioral response (CS+ and CS-), or the same behavioral response but different CS (Lick and No Lick), we examined the pairwise correlations of peak tone response magnitude between each corresponding trial type (**Fig. 2F**). Although all responses were found to be significantly correlated, we found that Lick trials (False Alarm and Hit) had the highest correlation in peak response magnitude for both glutamatergic (r=0.9) and GABAergic (r=0.92) neurons. Next, we verified the proportion of neurons that flipped from excitatory peak response activity to inhibitory response activity or vice versa, which provided us with a secondary measure of similarity of neuronal response. We found that Lick trials had the highest similarity with 0 neurons flipping signal of activity for both GABAergic and Glutamatergic neurons, while No Lick trials (Miss and Correct Rejection) trials had the greatest proportion of neurons that switched signs. Together this data suggests that adult mPFC neurons are activated or inhibited based on the behavior of the mouse, with the magnitude of the response being controlled by the CS presentation.

Adolescents have increase reward acquisition and drive compared to adults

To understand how adolescent mice encode reward predictive and no-reward predictive cues, we first had to assess the differences between adults and adolescents in our active reward task (**Fig. 3A**). Adolescent and adult mice were trained on the active reward task (**Fig. 3B**). We found that adolescents and adults learned simple associations (CS+ only) at a similar rate (**Fig. 3C**). However, with the addition of the CS- trials, adolescents choose different strategies for reward acquisition. Adolescents have more hit trials and a higher lick rate to hit trials compared to adults (**Fig. 3C**). Adolescent mice also had more false alarms outcomes than adults (**Fig. 3D**). However, adolescent mice had lower lick rates to tone during false alarms compared to hits ,suggesting that the adolescents have some understanding that the CS- is not rewarded. Together, this data corroborates our previous understanding that adolescent mice have increased reward motivation compared to adults.

Adolescent neuronal representation of outcomes, increased activity on hit trials

We then used 2-photon imaging to record calcium activity of adolescent mice as they perform the active reward task (**Fig. 4A**). Data was recorded and task-relevant neurons were identified as previously described for figure 2. We recorded a total of 2117 neurons, 1394 of which were found to be task-relevant (65.8%), meaning that they were significant for at least one of 3 predictors (CS+, CS-, Lick) used in the GLM (**Fig. 4B**). Furthermore, out of the task-relevant neurons 1198 were identified as glutamatergic, while 196 were GABAergic. When observing the mean activity of all the task-relevant neurons, we found that glutamatergic neurons had a significantly greater mean activity during hit outcomes compared to each of the other outcomes (miss, correct rejection, and false alarm; **Fig. 4C Top**). GABAergic neurons also exhibited increased mean tone activity during hit outcomes, when compared to miss and correct rejections, the trial outcomes where mice do not lick (**Fig. 4C Bottom**). For GABAergic neurons, false alarm outcomes were found to have significantly higher activity than correct rejection trials in adolescents. This data suggests that, in general, adolescent glutamatergic and GABAergic neurons tend to have the highest mean activity when the outcome of a trial is a hit. This is qualitatively different from the results observed in adults, which tended to have higher mean activity during CS- (correct rejection and false alarm) trials.

Next, we sought to explore the stability of neuronal responses by measuring how their peak response magnitude varied by outcome (hit, miss, correct rejection, and false alarm) across trials of the same cue-type, or the same behavior (CS+, CS-, Lick, No Lick) (**Fig. 4D**). Similar to adults, adolescent mice had the highest correlations between outcomes where mice licked the spout during the tone presentation (glutamatergic: r = 0.9, GABAergic: r =0.93). Interestingly, we also observed that outcomes from CS- (correct rejection and false alarm) had lower correlation in adolescent mice, compared to adults. Similar to adults, analysis of the proportion of neurons (pie chart insets) that were excited during one outcome (positive mean), but inhibited by a different outcome (negative mean), revealed that neuronal responses during licked trials varied the least, with 0 neurons switching from excited to inhibited, or vice versa, for either glutamatergic (top) or GABAergic (bottom) neurons. The largest proportion of neurons were observed to flip from excited to inhibited, or vice versa, during CS+ of differing outcomes, for both glutamatergic and GABAergic neurons. This data suggests that adolescent neuronal activity have some commonalities to adult neuronal patterns, both have greatest stability in licked trials. However, it also revealed some very potentially stark differences in adolescent neuronal activity patterns, with increased neuronal activity during hit trials and decreased correlation in CS- trials, suggesting that adolescents may process CS- trials differently than adults.

Inhibition of GABAergic neurons leads to disparate effects in adolescents and adults
To understand how neuronal activity differed between adolescent and adults, we first directly compared the mean tone activity of adolescent and adult mice (**Fig. 5A**). Our analysis revealed stark differences in global tone responses between adolescent and adult animals. A 3-way ANOVA between age, outcome, and neuronal type, revealed age to be a significant predictor of differences, with a significant main effect of age and interactions between age and outcome, as well as age and neuronal subtype. In subsequent analysis, we found that adolescent mice had increased mean tone activity during hit outcomes compared to adults for both glutamatergic and GABAergic neurons. Glutamatergic neurons also exhibited increased tone responsiveness during correct rejections when compared to adults. Importantly, independent two-way ANOVAs performed for each of the two neuronal subtypes revealed that only GABAergic neurons had a significant main effect of age, although both neuronal classes were significant for interactions between age by outcome. Although the neuronal data shows clear age differences in activity by outcome, we wanted to test if differences in activity patterns would equate to differences in task involvement.

To directly test how mPFC neurons were impacting behavior, we used chemogenetics to inhibit GABAergic neurons (**Fig. 5B**) in the adult (**Fig. 5C**) or adolescent (**Fig. 5D**) brain. Our choice to inhibit GABAergic neurons, and not glutamatergic neurons, was guided by our findings in figure 5A, where a main effect of age was found in GABAergic neurons, but not in glutamatergic neurons. Consistent with previous reports [12], inhibition of GABAergic neurons in the adult mPFC decreased premature licking (licking during the ITI), the day after inhibition. We expanded on previous reports, now showing that inhibition of GABAergic neurons in adults also increases licking to hit and reward period the day after inhibition, but not the day of. Surprisingly, chemogenetic inhibition of GABAergic neurons in adolescent mice led to completely different effects. We found that inhibition of GABAergic neurons in the adolescent mPFC decreased lick rates in false alarm and post false alarm, on the same day of inhibition. This suggests that GABAergic neurons work to modulate licking at both ages, but the direction of the modulation differs. In adults, GABAergic neurons inhibit licking responses, while in adolescence they drive these responses. Furthermore, the timing of the effects suggests that GABAergic neurons in the adolescent mPFC are directly gating licking, while adult mPFC GABAergic neurons may be more involved in modifying lick rates through learning.

Adolescent mPFC does not adequately represent no-reward cues

How reward and no-reward cues are encoded in the adolescent brain and how this differs from adults is not known. From our previous analysis, we had found that adolescents had increased reward cue activity when mice obtained the trial correctly (hit). We also found that the two CS- outcomes (miss and correct rejection) had lower correlations in peak response magnitude compared to adults, which could be indicative of poor encoding of CS- cue, the commonality between the two outcomes. We therefore hypothesized that the adolescent mPFC may be encoding different information than the adult mPFC. Specifically, we thought that the adolescent mPFC may be better at encoding reward information but worse at encoding no-reward information. To begin testing our hypothesis, we examined if the number of neurons that made up our previously identified task-relevant neurons (as determined by a GLM) were similar across the different predictors (CS+, CS-, and Lick). In adults 26.0% of neurons are CS+ predictive, while 50.3% of neurons are CS+ predictive in adolescents (**Fig. 6A**). Further, 16.2% of adult neurons are CS- predictive whereas only 6.5 % of adolescent neurons were CS- predictive, while 3.9% of adult neurons and 4.2% adolescent neurons were lick predictive. When we break down the activity patterns by predictor and beta weight (**Fig. 6B**), we can then observe how adolescent and adult activity patterns for each subpopulation changes for each CS (**Fig. 6C**). We find that adolescents have greater activity in lick predictive neurons compared to adults. Second, CS- predictive neurons in adults have a rapid peak of mean activity, whereas adolescents do not (for full statistical analysis of mean, max, and time of max activity see supplementary figure 5).

To fully understand how well the neuronal populations encoding task-relevant information could predict CS identity (was the trial a CS+ trial or a CS- trial), we used a support vector machine (SVM) decoder (**Fig. 6D**). We trained decoders on 70% of trials from different populations of neurons and tested the model on the remaining 30% of trials for that same population. As control, we used all neurons (including non-task relevant neurons) to decode CS identity. For each analysis, 20 iterations, with randomly sampled trials, were used to assess replicability of our model. In adults, we found that SVM decoder trained on all neurons (task-relevant and non-task-relevant neurons) could successfully determine the identity of the CS in 74% of trials. Decoding with only CS+ and CS- predictive neurons, as determined by a GLM, increased the performance of the GLM. While decoding with only CS- or only CS+ predictive neurons did not hinder or enhance performance. However, in adults, SVM decoding efficiency decreased when only lick predictive neurons were used, and removing either CS+ or CS- predictive neurons from the global neuronal pool diminished decoding ability. Adolescent neurons however, seemed to be carrying different information. First, adolescent Lick predictive neurons were sufficient to decode CS identity at similar levels to all neurons, CS+ and CS- predictive neurons together, and CS+ neurons only. In fact, Lick predictive neurons outperformed CS- predictive neurons in their decoding ability, despite Lick neurons being a smaller population of neurons. However, Lick neurons did not prove necessary for decoding CS identity in adolescents, CS+ neurons did. Removing CS+ neurons (no CS+) from the global adolescent neuronal pool decreased decoding efficacy of the SVM. Even more important, removing CS- (no CS-) from the global adolescent neuronal pool did not decrease decoding efficiency. Together, this analysis suggests that adolescent neurons may not be adequately representing CS- through CS- tone responsive neurons, instead preferentially encoding information in lick responsive and CS+ responsive neurons. This over reliance on CS+ and lick behavior encoding may explain why adolescent mice have trouble withholding licks when a CS- is presented.

Lastly, we sought to visualize and analyze if task-relevant neurons showed differences in activity depending on task outcome (**Fig. 7A**). We averaged the neuronal activities based on the GLM predictor they were significant to, and their beta weights (**Fig. 7B**). When neurons were

grouped by predictor, we observed large age differences between activity patterns of different outcomes, including in the peak activities, the time of peak activity and the mean activity of many populations (**Fig. 7C** and **7D**; for statistical analysis see supplementary figure 7). For example, we observed that adolescents have a greater mean tone activity in + beta weight CS+ predictive neurons, compared to adults (**Fig. 7E**). Whereas this same + beta weight CS+ population is decreased in adolescents during correct rejections, compared to adults. Together this data suggests that the adolescent and adult mPFCs represent task outcomes differently.

Discussion

A growing body of work now suggests that critical periods in postnatal development can alter circuit development and increase the propensity of numerous psychiatric disorders [22,23]. Specifically, adolescence, represents both the onset of numerous psychiatric disorders including substance use disorder, depression, obsessive-compulsive disorder, and attention deficit hyperactivity disorder [2], and is a unique period for reward motivation and reward-seeking, with numerous studies suggesting that adolescent humans and mice exhibit increased reward-motivated behaviors during this age period [3–8]. Changes in reward motivation have been identified as a main symptom of psychiatric disorders such as depression, obsessive-compulsive disorder, and attention deficit hyperactivity disorder [1]. Recent animal studies in adults have shown that the mPFC is involved in reward learning and expression [9,11,24]. However, a large body of work shows that the adolescent mPFC is still undergoing developmental changes, as inhibitory neurons continue differentiating, dendritic arborization grows, excitatory neurons undergo pruning, and receptor expression densities shift [17–19,25–27]. Although numerous anatomical changes have been identified in the adolescent circuit, how these alter communication at the circuit-level to produce adolescents' increase in reward motivation had not been delineated. Our findings now delineate various mechanisms that account for adolescent reward motivation. At a behavioral level, we found that adolescent mice respond to more reward and no-reward cues, but differences in lick rates to both cues indicate that adolescents understand the cues as signaling different events. When assessing neuronal activity, we found that the adolescent mPFC over-represents reward predictive cues (CS+) and under-represents non-reward predictive cues (CS-), when compared to adults. Furthermore, using support vector machine decoders, we tested if different subsets of neurons could decode the identity of the CS (CS+ versus CS-). Adolescents had fewer no-reward (CS-) encoding neurons, and removal of these neurons did not decrease model performance, as it did in adults. Together, the data suggest that adolescents may not be able to fully interpret, or ignore, the no-reward cues, leading to reward-seeking even when no rewards are available. This diminished ability to encode no-reward cues may be why adolescents appear more driven to obtain rewards.

In the mPFC, GABAergic neurons exert their function on the microcircuit through inhibition and disinhibition. In adults, inhibition of parvalbumin interneurons disinhibits glutamatergic projection neurons to gate behavior [28,29]. However, during adolescence parvalbumin neurons are still maturing, increasing in both density and dendritic arborization, possibly leading to differences in the disinhibition network [13,20,30–32]. Consistent with previous studies, we found that GABAergic mPFC neurons drive non-specific licking (pre-tone licking) in adults. However, in adolescence, we found that GABAergic inhibition did not alter non-specific licking. Instead, GABAergic neurons in the adolescent mPFC seemed to drive licking to no-reward cues. Further, adolescent glutamatergic and GABAergic neurons both displayed increased activity to rewarded cues when mice obtained the trial correctly. Unlike in adults, adolescent GABAergic activity was greater than glutamatergic activity during hit and false alarm outcomes, providing evidence that the inhibition/disinhibition networks function differently in adolescence. As GABAergic neurons are

still developing and altering their function, projections to the mPFC that send reward-related information (e.g. from ventral tegmental area) are also maturing [33–35], possibly relaying different information in both magnitude and temporal dimensions to both GABAergic and glutamatergic neurons. These changes in anatomical connectivity are likely all contributing to the stark differences in the mPFC microcircuit we observed here. Future studies should focus on mapping how development is altering inhibition/disinhibition networks to bias the adolescent mPFC to overrepresent and overseek reward opportunities.

Figures

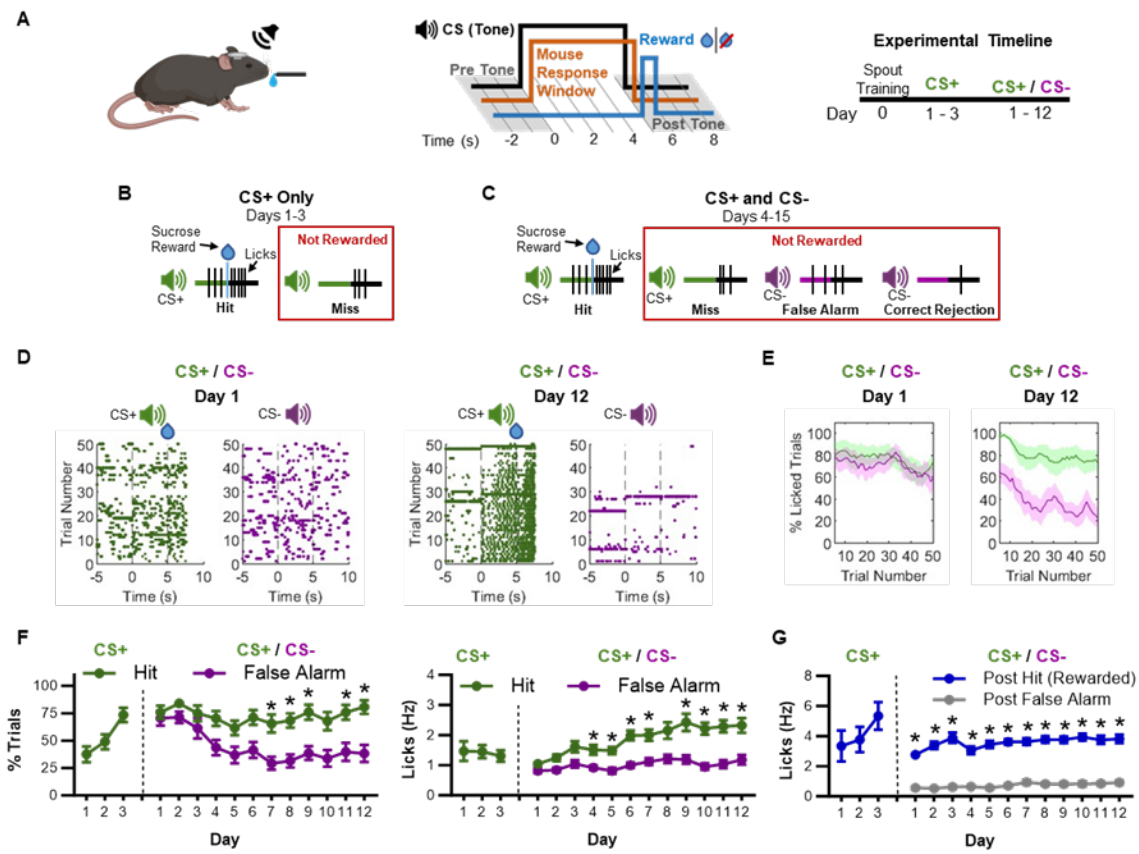

Figure 1: An active reward task for head-fixed mice

A) Picture of head-fixed mouse acquiring a sucrose reward (left), schematic of trial sequence (middle), and general experimental training timeline (right).
B) Schematic of CS+ only training sessions (3 days of training) where mice learn to lick the spout during CS+ presentations to obtain a reward at CS+ tone offset.
C) Schematic of CS+ and CS- training session where mice can obtain a reward at tone offset if they lick the spout during CS+ presentations but not during CS- presentations.
D) Summary of licking behavior. Left: rasterized lick times for an example session of day 1 of CS+/CS- session aligned to tone onset (set as time point zero), if rewarded, sucrose droplet is delivered at tone offset (at 5s). CS+ trials appear in green, CS- trials appear in magenta. Right: Rasterized lick time for the last day of training for an example adult mouse.
E) Example within day data for the first (left) and last day (right) of CS+/CS- training of adult mice. CS+ trials appear in green, CS- trials appear in magenta. Data is shown as a moving window of 5 consecutive trials from within the same session. Dark line is mean, sem is presented as the shaded area.
F) Graph of adult mice's trial acquisition (left) and lick rates (right) during CS+ only and CS+/CS- training sessions. If a mouse licks at least one time during the CS+, the trial is categorized as a hit, If they lick at

least once during the CS-, the trial is categorized as a false alarm. During CS+/CS- training, a two-way repeat measure ANOVA revealed that adult mice had significant differences in the % trials they acquire by CS type ($F_{1,28} = 18.36$, $p = 0.0002$), and across days ($F_{4.7,132.8} = 6.41$, $p < 0.0001$), with a significant day by CS type interaction ($F_{11,308} = 2.36$, $p = 0.0081$). A Sidak's multiple comparison analysis for each day of CS+/CS- training revealed that trial acquisition becomes significantly different by day 7 of training ($p < 0.05$). We then used a mixed-effects model to test for differences in lick rate during CS+/CS- training. We found a main effect of CS type ($F_{1,28} = 33.71$, $p < 0.0001$), day of training ($F_{4.9,137.5} = 10.41$, $p < 0.0001$), and an interaction between day by CS type ($F_{11,306} = 3.72$, $p < 0.0001$). A multiple comparison revealed that lick rates between false alarms and hits were significantly different starting on day 4 ($p = 0.040$) of CS+/CS- training. Data in shown as mean ± SEM, * indicates $p < 0.05$ on a Sidak's multiple comparison post hoc test. n = 11-15 mice.

G) Graph of lick rates to sucrose reward (5 seconds post hit trials) compared to the 5 second post false alarms. During CS+/CS- training, mice have increased lick rates at tone offset in hits, where they receive a sucrose reward, compared to post false alarms, where no reward is delivered ($F_{1,28} = 229.8$, $p < 0.0001$). A significant effect of day of training was also observed ($F_{5.4,151.9} = 4.44$, $p = 0.0006$). Data in shown as mean ± SEM, * indicates $p < 0.05$ on a Sidak's multiple comparison post hoc test. A mixed-effects model was used to analyze main effects. n = 11-15 mice. Data for Post Correct Rejections and Post Miss are found in the supplemental figure 1.

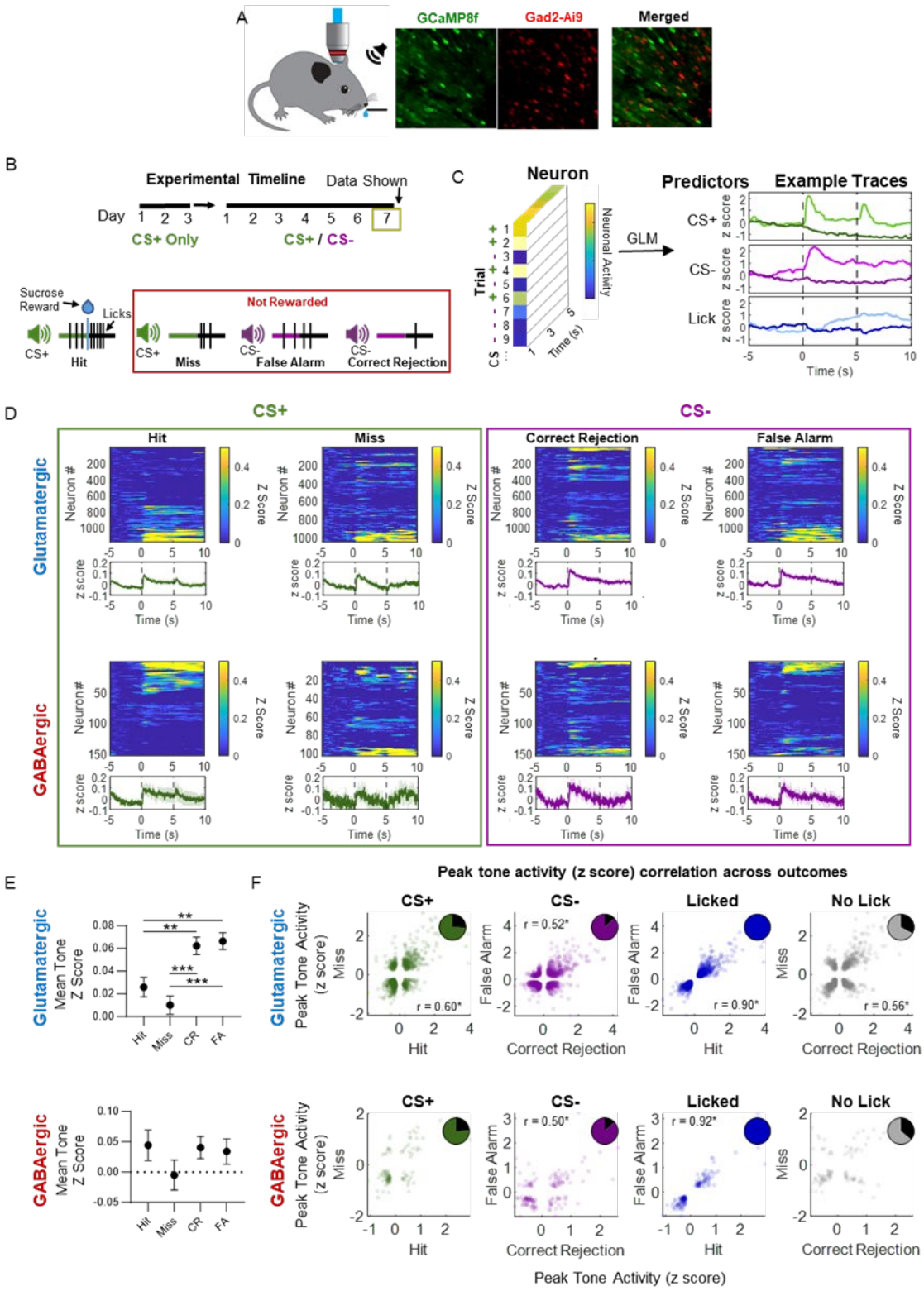

Figure 2: Neuronal co-encoding of behavioral response and stimuli presentation

A) Cartoon of mouse during 2P imaging of the mPFC and representative images of glutamatergic (green only) and GABAergic (co-labeled green and red) neurons during 2P imaging. Images were captured using Galvano imaging and processed using a max intensity projection. Neurons were recorded from 5 adult mice.

B) Experimental timeline of behavioral training. 2P imaging data was extracted from day 7 of CS+/CS- training. Schematic of the different CS outcomes during CS+/CS- training sessions.
C) Schematic of generalized linear model (GLM) used to classify neurons. 3 predictors were used: CS+, CS-, and Lick. Only Pre-tone and Tone activity (-5 to 5 seconds) was used in the GLM.
D) Heatmap of neuronal activity for all neurons that are significant in the GLM. Neurons are sorted by hierarchical binary cluster tree based on the Euclidean distance between neuronal traces. The average neuronal trace (average of all neurons in the heatmap) is presented below.
E) Plot of mean tone activity (0 to 5 seconds) for each outcome for glutamatergic (top) and GABAergic (bottom) neurons. For glutamatergic neurons, outcomes were found to be significantly different ($F_{3, 4594} = 11.81$, $p < 0.0001$), with Hit and Miss trials having lower mean tone activity compared to Correct Rejection (Hit: $p = 0.0057$; Miss: $p < 0.0001$) and False Alarm trials (Hit: $p = 0.0015$; Miss: $p < 0.0001$). No significant effects were observed in GABAergic neurons. One-way ANOVA followed by Tukey's multiple comparison analysis was used to analyze mean tone activity differences between outcomes. Data is shown as mean ± SEM.
F) Pairwise correlations of neuronal activity by trial outcome for each CS (CS+ and CS-), and behavior (Licked or No Lick). Each point represents the peak tone response magnitude (positive or negative) of a glutamatergic (top) or GABAergic (bottom) neuron in a given trial type. Only task relevant neurons (GLM significant) are plotted. Linear coefficient of correlation (r) is presented on each graph, with * indicating a significant correlation ($p < 0.05$). Licked trials (False Alarm and Hit) have the highest correlations for both Glutamatergic and GABAergic neurons. Pie chart insets display the percent of neurons that showed a sign reversal in their peak response magnitude (black wedges), indicating a transition from inhibition (negative values) to excitation (positive values), or vice versa. The colored wedges represent the percent of neurons whose activity remained in the same direction (both inhibited or both excited) for both outcomes. Glutamatergic neurons exhibited sign reversal in their peak response magnitude during CS+ (25.4%), CS- (13.1%), and No Lick (32.9%) trials; GABAergic neurons exhibited sign reversal during CS+ (24.2%), CS- (12.9%), and No Lick (35.9%) trials. No neuron exhibited sign reversal during Licked trials. (see supplement for graph and additional statistics). Statistics for all other comparisons, and analysis of distribution of peak activity and time of peak activity are found in the supplemental figure 2.

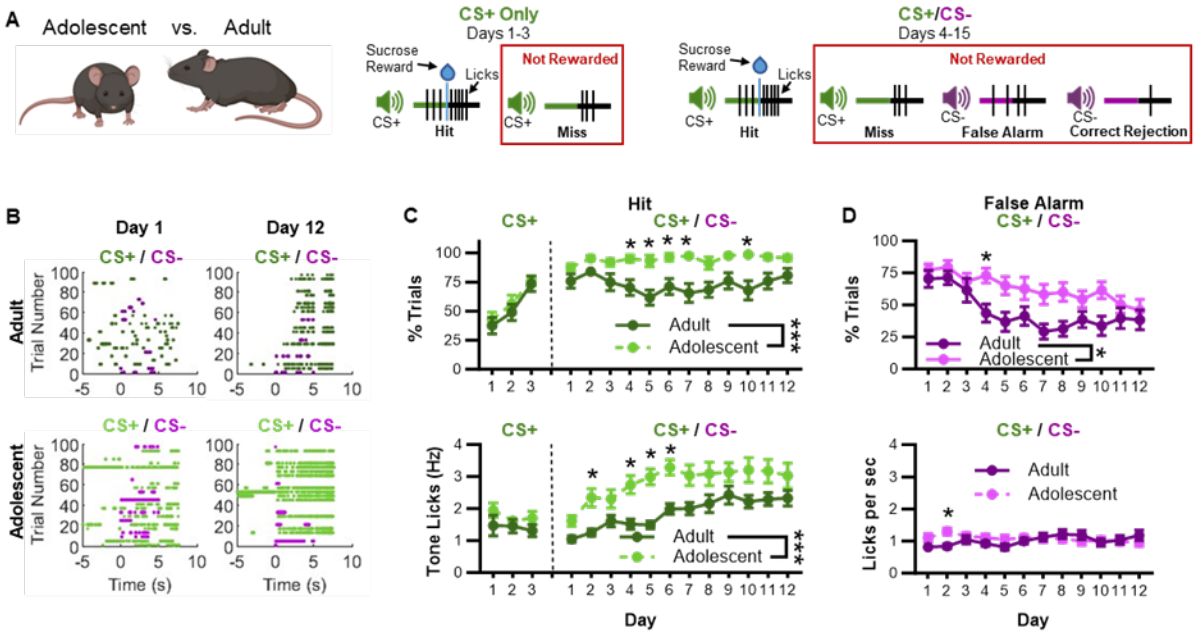

Figure 3: Adolescent mice have increased reward motivation

A) Cartoon picture of adolescent versus adult mice (left), schematic of CS+ only training sessions where mice learn to lick the spout during CS+ presentations to obtain a reward at CS+ offset (middle), and schematic of CS+/CS- training session where mice can obtain a reward at tone offset if they lick the spout during CS+ presentations but not during CS- presentations (right).
B) Example trials of lick behavior. Rasterized lick times for an example session on day 1 (left) and day 12 (right) of CS+/CS- training, aligned to tone onset (set as time point zero). If rewarded, a sucrose droplet is delivered at tone offset (at 5s). CS+ trials appear in green, CS- trials appear in magenta. Top raster plots are an example of an adult mouse, while bottom raster plots show an example of an adolescent mouse. Only 25 of the 100 trials (every 4th trial) are shown for ease of visualization.

C) Comparison of adults and adolescents for % acquired CS+ trials (top) and CS+ lick rates in hit trials (bottom). Adolescent mice have significantly more hit trials (CS+ trials where they lick) compared to adults ($F_{1,26} = 21.70$, $p < 0.0001$). Adolescent mice also showed a greater tone lick rate during hit trials compared to adults ($F_{1,26} = 15.27$, $p = 0.0006$). A further main effect of training day was found for tone lick rates ($F_{3.8,99.7} = 12.11$, $p < 0.0001$), with lick rates increasing with training. Data is shown as mean ± SEM, * indicates $p < 0.05$ on a Sidak's multiple comparison post hoc test. Main effects were determined with a two-way repeat measure ANOVA. n = 10-15 mice per age group.

D) Comparison of adults and adolescents for % incorrectly acquired CS- trials (top) and CS- lick rates in false alarm trials (bottom). A two-way repeated measure ANOVA demonstrated that adolescent mice have significantly more false alarm trials (CS- trials where they lick) compared to adults ($F_{1,26} = 7.16$, $p = 0.012$). A main effect of training day was also found for the % of false alarms ($F_{4.6,121.5} = 9.59$, $p < 0.0001$), with the number of false alarms decreasing with training. However, a mixed-effects model analysis showed that adolescent mice do not generally have an elevated lick rate during false alarm trials compared to adults ($F_{1,26} = 0.49$, $p = 0.48$), although a significant interaction of age by training day was observed ($F_{11,284} = 2.15$, $p = 0.016$). Data in shown as mean ± SEM, * indicates $p < 0.05$ on a Sidak's multiple comparison post hoc test. n = 10-15 mice per age group.

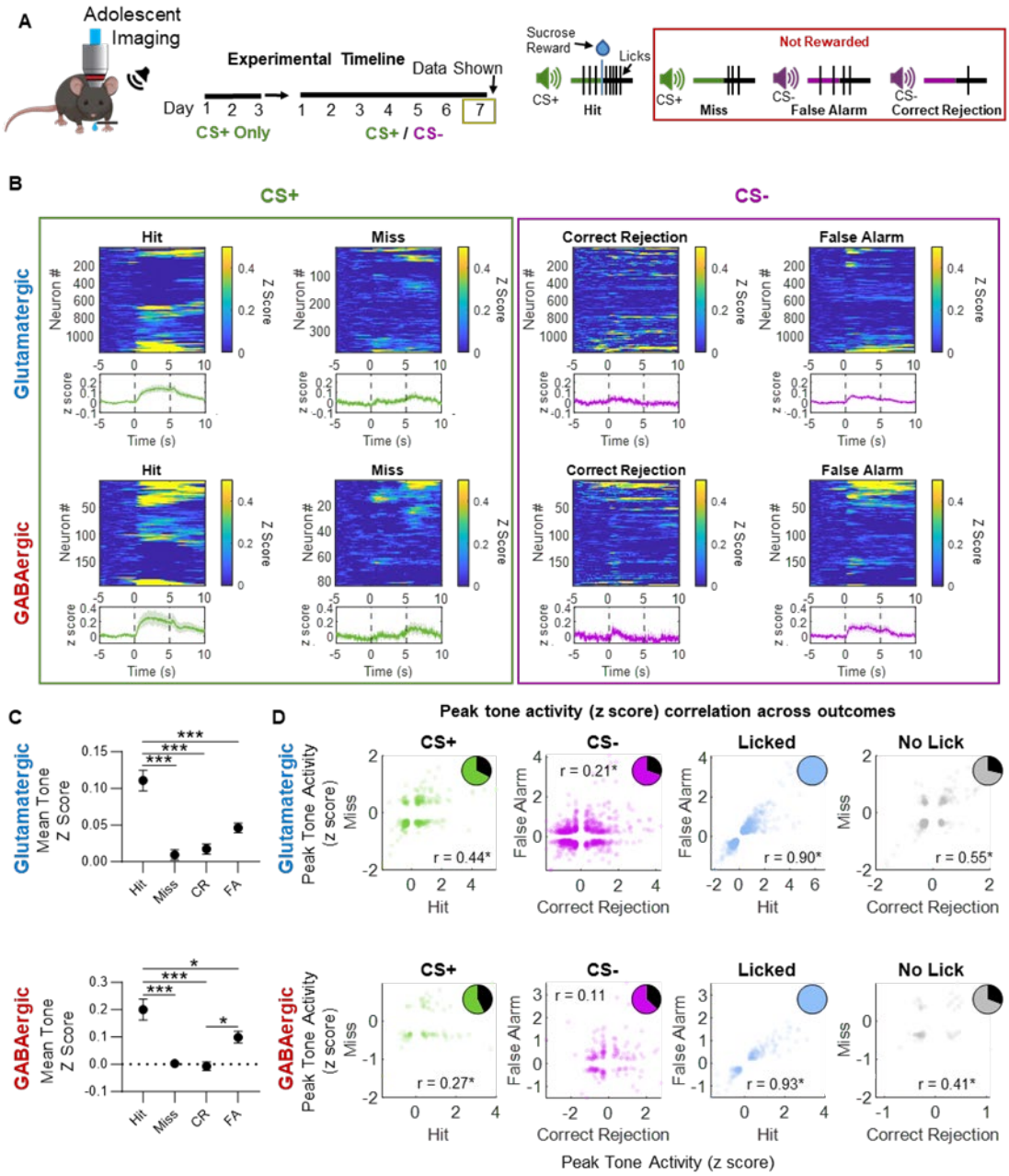

Figure 4: Neuronal encodings of task outcomes within the adolescent mPFC

A) Experimental timeline of behavioral training. 2P imaging data was extracted for day 7 of CS+/CS- training, and schematic of the different CS outcomes during CS+/CS- training sessions. Neurons were recorded from 4 adolescent mice.

B) Heatmap of neuronal activity for all task-relevant neurons (significant in the GLM). Neurons are sorted by hierarchical binary cluster tree based on the Euclidean distance between neuronal traces. Each trial outcome (hit, miss, correct rejection, and false alarm) are sorted independently. Each row represents a neuron, with traces aligned to tone onset (set as time point zero). For hit trials, sucrose reward is delivered at tone offset (at 5s). The average neuronal trace (average of all neurons in the heatmap) is presented below.

C) Plot of mean tone activity (0 to 5 seconds) for each outcome for glutamatergic (top) and GABAergic (bottom) neurons. For glutamatergic neurons, outcomes were found to be significantly different ($F_{3, 3969} = 19.84$, $p < 0.0001$), with Hit trials having increased mean tone activity compared to Miss ($p < 0.0001$), Correct Rejection ($p < 0.0001$) and False Alarm trials ($p < 0.0001$). Similarly, in GABAergic neurons, mean tone

activity was found to significantly vary by outcome ($F_{3, 668} = 12.69$, $p < 0.0001$), with Hit trials having higher tone activity compared to Miss ($p = 0.0002$), Correct Rejection ($p < 0.0001$), and False Alarm ($p = 0.026$) trials. GABAergic neurons also had greater activity during False Alarms compared to Correct Rejections ($p = 0.017$). One-way ANOVA followed by Tukey's multiple comparison analysis was used to analyze mean tone activity differences between outcomes. Data is shown as mean ± SEM.

D) Pairwise correlations of neuronal activity by trial outcome for each CS (CS+ and CS-), and behavior (Licked or No Lick). Each point represents the peak tone response magnitude (positive or negative) of a glutamatergic (top) or GABAergic (bottom) neuron in a given trial type. Only task relevant neurons (GLM significant) are plotted. Linear coefficient of correlation (r) is presented on each graph, with * indicating a significant correlation ($p < 0.05$). Licked trials (false alarm and hit) have the highest correlations for both Glutamatergic and GABAergic neurons, while CS- trials (false alarm and correct rejection) have the lowest. Pie chart insets display the percent of neurons that showed a sign reversal in their peak response magnitude (black wedges), indicating a transition from inhibition (negative values) to excitation (positive values), or vice versa. The colored wedges represent the percent of neurons whose activity remained in the same direction (both inhibited or both excited) for both outcomes. Glutamatergic neurons can be observed to flip their peak response magnitude from positive to negative (or vice versa) during CS+ (32.7%), CS- (30.3%) and No Lick (28.7%) trials; GABAergic neurons during CS+ (42.8%), CS- (36.7%) and No Lick (30.9%) trials. No neuron exhibited sign reversal during Licked trials. Statistics for all other comparisons, and analysis of distribution of peak activity and time of peak activity are found in the supplemental figure 3.

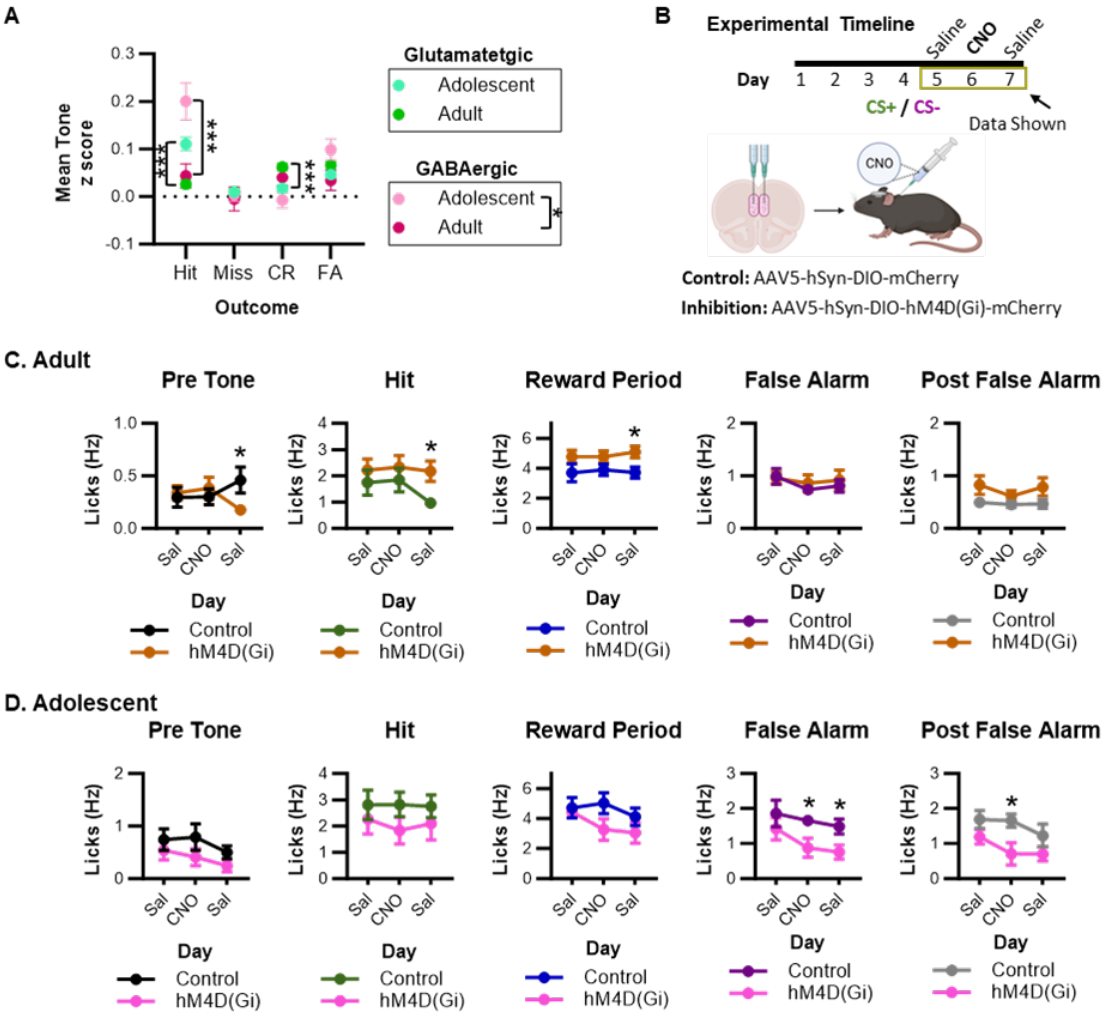

Figure 5: GABAergic neurons are required for licking to non-rewarding cues in adolescence, but not in adults

A) Analysis of the mean tone activity for adult and adolescent glutamatergic and GABAergic neurons in hit, miss, correct rejection (CR) and false alarm (FA) trials. A three-way ANOVA for age, outcome, and cell type revealed that age was a main source of variation ($F_{1,9792} = 6.88$, $p = 0.0087$). Significant main interactions

of age by outcome ($F_{3, 9792} = 16.14$, $p < 0.0001$), and age by cell type ($F_{1, 9792} = 4.54$, $p = 0.033$), and outcome by cell type ($F_{3, 9792} = 3.63$, $p = 0.012$) were also observed. A main effect of Outcome was also observed ($F_{3, 9792} = 16.62$, $p < 0.0001$), indicating that neurons displayed differences in tone responses for the differing trial types. Follow-up two-way ANOVAs were conducted for each of the two neuronal subtypes (glutamatergic and GABAergic). In glutamatergic neurons, we found a main effect of outcome ($F_{3, 8563} = 11.11$, $p < 0.0001$) and an interaction between outcome and age ($F_{3, 8563} = 21.48$, $p < 0.0001$). Glutamatergic mean tone activity was significantly different between adolescent and adult mice during hit ($p < 0.0001$) and correct rejection trials ($p = 0.0009$). For GABAergic neurons, a main effect of age ($F_{1, 1229} = 5.77$; $p = 0.016$), outcome ($F_{3, 1229} = 8.80$; $p < 0.0001$), and interaction of age by outcome were detected ($F_{3, 1229} = 6.21$; $p = 0.0003$). Hit trial activities were found to significantly differ between adolescent and adult GABAergic neurons ($p < 0.0001$).

B) Experimental timeline and design for GABAergic inactivation using chemogenetics. Experimental mice (Gad2-cre) were injected with virus coding for chemogenetic inhibition channels (DIO-hM4D(Gi)-mCherry), control mice were injected with a virus lacking the chemogenetic channel (DIO-mCherry). Mice were trained on the CS+/CS- for 4 days. On day 5 of training, mice were injected with saline for the pre-test; on day 6, all mice (control and experimental) were injected with DREADDs agonist CNO (0.3 mg/kg) for the test; and on day 7, all mice were injected again with saline for the post-test. Additionally, we tested the effects of GABAergic inactivation on learning simple associations (CS+ only), which you can find in supplementary figure 4.

C) Multiple t test comparisons were performed to test for effects on each day of training. For adult inhibition of GABAergic neurons, we found that chemogenetic inhibition on day 6 of training did not have any significant effects. However, when giving the posttest (day 7), we found that hM4D(Gi) mice had increased lick rates during hit ($t_{22} = 2.84$; $p = 0.0095$) and reward period (post hit; $t_{22} = 2.51$; $p = 0.019$) epochs. N = 10-12 per group. Data in shown as mean ± SEM, * indicates $p < 0.05$

D) Multiple t test comparisons were performed to test for effects on each day of training. For adolescent inhibition of GABAergic neurons, we found that chemogenetic inhibition on day 6 of training reduced lick rates during false alarms ($t_{10} = 2.29$; $p = 0.044$) and post false alarms ($t_{10} = 2.27$; $p = 0.046$). Reduction in lick rates observed during false alarm lasted until the following day ($t_{10} = 2.42$; $p = 0.035$). N = 5-7 per group. Data in shown as mean ± SEM, * indicates $p < 0.05$

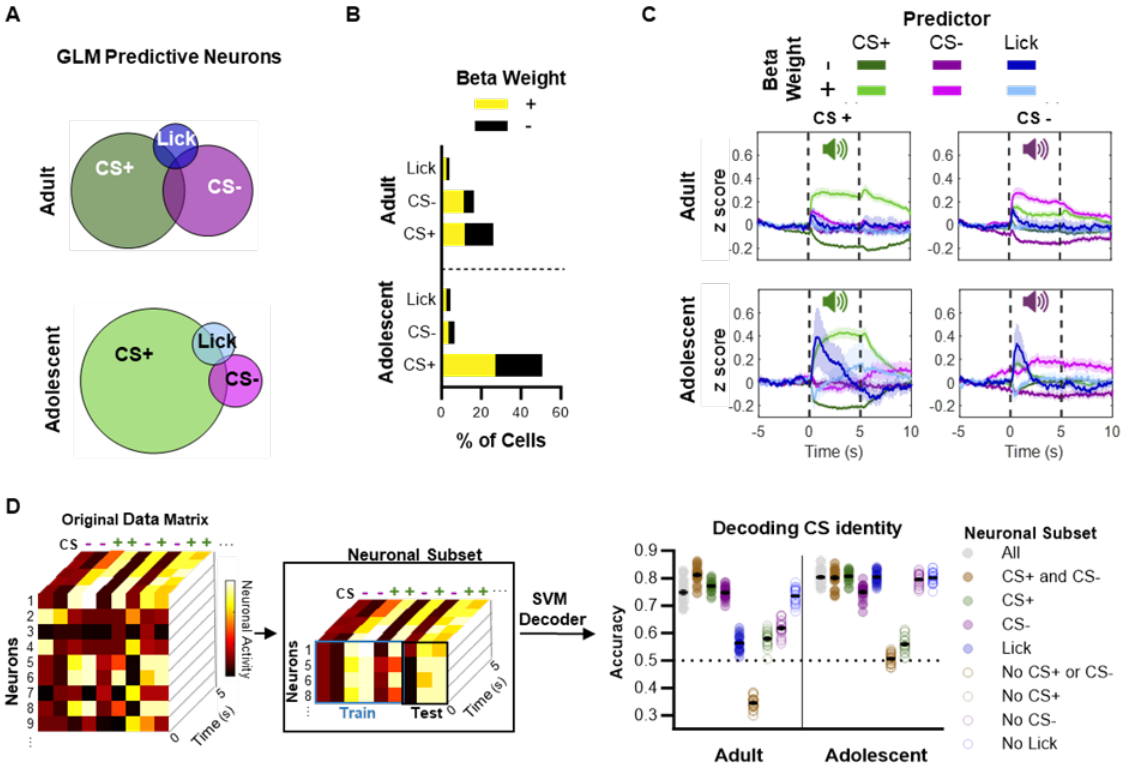

Figure 6: Decoding ability of subpopulations of neurons demonstrate adolescent bias toward reward cue predictive encoding.

A) Venn diagram of the proportion of mPFC glutamatergic neurons significant for each predictor (CS+, CS- and/or Lick) in the GLM described for adult (top; see figure 2), and adolescent (bottom; see figure 4) mice.
B) Percent glutamatergic neurons in adult and adolescent mice significant for a given predictor by the sign of their corresponding GLM beta weights (positive or negative). Neurons that were significant for more than one predictor appear more than once.
C) Mean neuronal activity of glutamatergic neuronal populations significant for each predictor during CS+ (left) and CS- (right) trials, for adult (top) and adolescent (bottom) mice. Neurons were grouped according to their beta weight sign (positive or negative). Graphs show mean (dark line) ± SEM (shaded area). Statistical comparisons of the means can be found in supplemental figure 5.
D) Decoding efficiency of CS+ versus CS- trials by distinct neuronal subpopulations in adult and adolescent mice. Schematic of SVM decoding of neuronal subpopulations (left). SVMs were run on matrices containing glutamatergic and GABAergic neurons from 4-5 mice. In adults, all tested neuronal subsets were able to decode CS+ versus CS- trials when compared to SVM decoding of shuffled CS label data. For adolescent mice, CS- neuronal subset was the only subset found to be not significant when compared to shuffled data ($t38 = 2.02$, $p = 0.0502$). A Tukey multiple comparison analysis was used to determine which subsets performed significantly better or worse than the subset that contained all neurons (labeled All in the graph). In adults, CS+ and CS- neuronal subset performed better than the All neuron subset ($p < 0001$). The No CS+ ($p < 0001$), No CS- ($p < 0001$), No CS+ or CS- ($p < 0001$), and Lick ($p < 0001$) subsets performed worse than the neuronal subset containing all neurons. In adolescents, CS- ($p < 0001$), No CS+ ($p < 0001$), and No CS+ or CS- ($p < 0001$) subsets performed worse than the neuronal subset containing all neurons. Lastly, we compared the performance of all adolescent neurons compared to all adult neurons and found that the adolescent neurons could decode the identity of the CS better than the adults ($p < 0001$). Individual values represent one decoding test. Only the 5 seconds of tone activity was used for decoding. 20 train / test sessions were run for each subpopulation. For each run, the 120 CS trials were randomly shuffled, with time series remaining intact. Individual runs and mean ± SEM for the decoder is shown. Significance from shuffled was tested with Holm-Sidak multiple comparison analysis. * indicates $p < 0.05$ on a Sidak's multiple correction post hoc test. For comparison of decoding compared to shuffled data see supplemental figure 6.

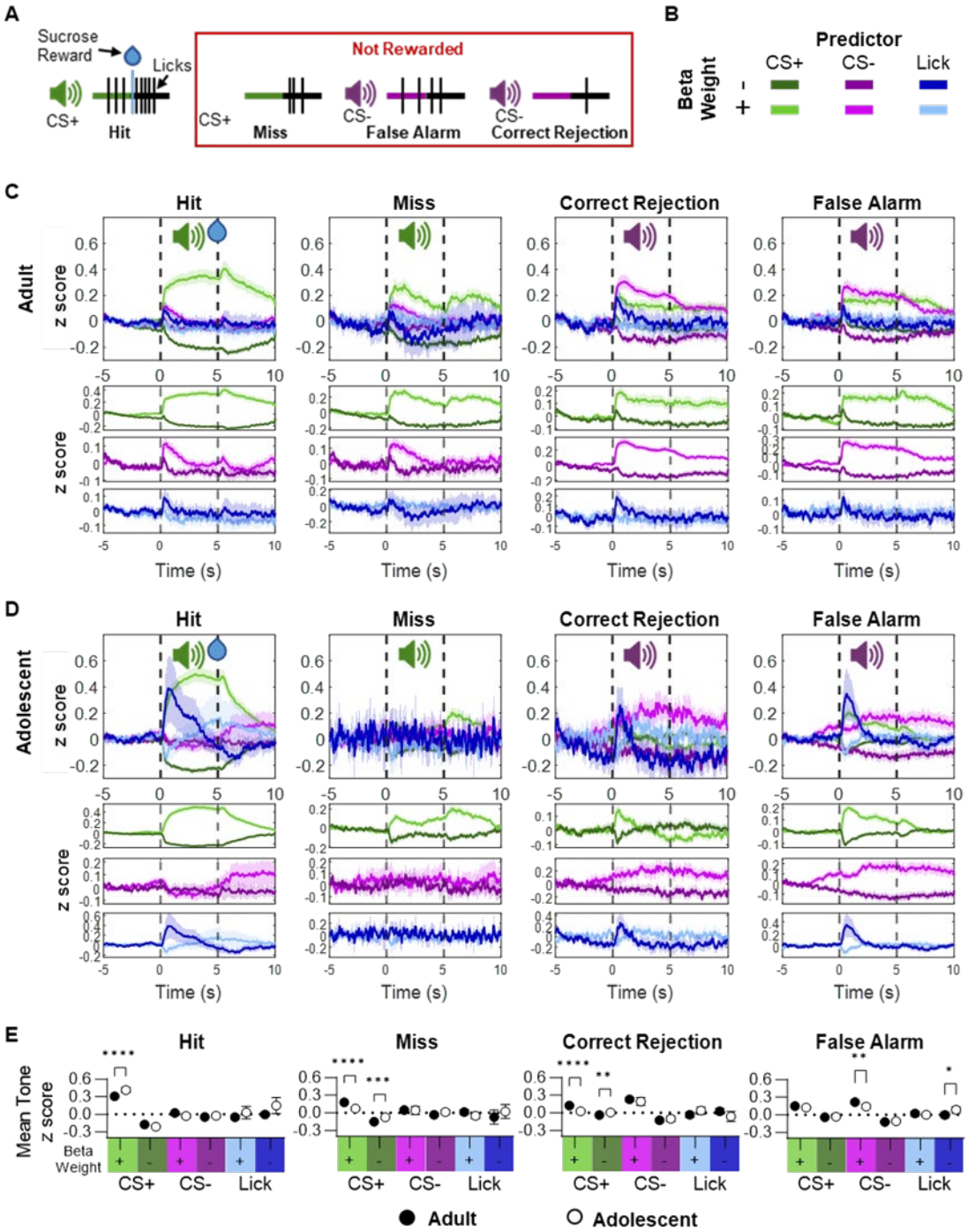

Figure 7: mPFC neuronal subpopulation activity changes across outcomes.

A) Schematic of the different CS outcomes during CS+/CS- training sessions.

B) Figure legend for panels C, D, and E. Shows the color coding for subpopulations of neurons divided by the predictor (CS+, CS-, and Lick) and beta weights (positive or negative).

C) Mean activity for neuron subpopulations in adults across outcomes (hit, miss, correct rejection and false alarm). Top graphs show an overlay of mean subpopulation activity for visual comparison. Bottom 3 graphs display subpopulations significant for each predictor in more detail (CS+: green; CS-: magenta; and Lick: blue). Graphs show mean ± SEM (shaded area).

D) Mean activity for neuron subpopulations in adolescents across outcomes. Top graphs show an overlay of mean subpopulation activity across outcomes. Bottom 3 graphs show subpopulations significant for each

predictor in more detail (CS+: green; CS-: magenta; and Lick: blue). Graphs show mean ± SEM (shaded area).

E) Mean tone activity of subpopulations presented in panels C and D. A two-way ANOVA was used to analyze each outcome for a main effect of age, neuronal subset, and interaction between age and neuronal subset. A main effect of age was only found for hit ($F(1, 2575) = 5.694$, $p = 0.017$). While a main effect of neuronal subset (hit: $F(5, 2575) = 266.9$, $p < 0.0001$; miss: $F(5, 1528) = 57.54$, $p < 0.0001$; correct rejection: $F(5, 2575) = 57.70$, $p < 0.0001$; false alarm: $F(5, 2575) = 102.1$, $p < 0.0001$), and interaction between neuronal subset by age (hit: $F(5, 2575) = 5.814$, $p < 0.0001$; miss: $F(5, 1528) = 8.791$, $p < 0.0001$; correct rejection: $F(5, 2575) = 9.103$, $p < 0.0001$; false alarm: $F(5, 2575) = 2.893$, $p = 0.013$) was found for all four outcomes. During hit trials, we found that adolescent mice had increased mean activity in positive beta weight CS+ neurons compared to adults ($p < 0.0001$). During miss and correct rejection trials, adolescent mice had decreased mean tone activity in positive beta weight CS+ neurons (miss: $p < 0.0001$; correct rejection: $p < 0.0001$) and increased mean tone activity in negative beta weight CS+ neurons (miss: $p = 0.0005$; correct rejection: $p = 0.0089$) compared to adults. During false alarms, adolescent mice had decreased mean tone activity in positive beta weight CS- neurons ($p = 0.0054$) and increased mean tone activity in negative beta weight Lick- neurons ($p = 0.037$) compared to adults. Mean ± SEM are shown. For analysis of peak activity and time of peak activity, and differences between subpopulations, see supplemental figure 7.

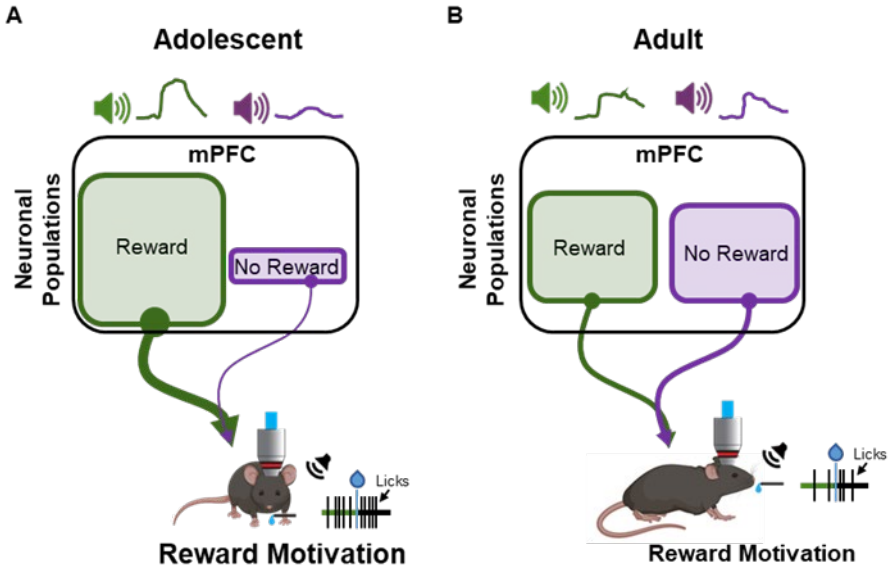

Figure 8: Proposed model for mPFC driven increased adolescent reward motivation

A) Adolescent mice have overrepresentation of CS+ encoding neurons, and underrepresentation of CS- encoding neurons within the mPFC. This leads to increased reward-motivated behavior in adolescence, indexed by increased licking.

B) In adults, the CS- encoding population is smaller than the CS+ encoding population, but much larger than the CS- encoding population in adolescents. This balance between CS+ and CS- encoding neurons allows the adult to better control when they will lick, decreasing overall lick rates and allowing them to withhold licks to non-rewarding cues.

Materials and Methods Summary

Subjects

Male and female C57BL/6 wildtype (Charles River Laboratories) were used for behavioral experiments. For 2-photon imaging Gad2-Cre (*Gad2tm2(cre)Zjh*/J, JAX#010802) [36] homozygous mice were crossed with Ai9 homozygous reporter mice (B6.Cg-*Gt(ROSA)26Sor*$^{tm9(CAG\text{-}tdTomato)Hze}$/J, JAX#007909) [37] to produce heterozygous mice that expressed tdtomato in Gad2 (inhibitory) neurons. Heterozygous Gad2-Cre mice were used for chemogenetic inhibition of GABAergic neurons. Transgenic mouse lines were derived from a

breeding stock acquired from Jackson Laboratories. All animals were housed according to NIH guidelines and maintained on a 12-hour light:dark cycle. Mice had free access to water and food except during experiments where mice underwent water restriction (see Active Reward Task section). Mice were weaned at P21 and group housed with littermates. Animal procedures are approved by Weill Cornell Medical College Institutional Animal Care and Use Committee, and consistent with the National Institutes of Health Guide for the Care and Use of Laboratory Animals.

Behavioral Manipulations and Testing

General

For assessing developmental changes in neuronal activity during reward learning and expression we used a head fixed modified pavlovian reward task (active reward task). Mice were trained through 3 phases: spout training (1 day, two 30 min. sessions), CS+ training (3 days, 1 session per day), and CS+/CS- training (7-12 days, 1 session per day). During spout training, mice are trained to lick sucrose (~8uL of 10% sucrose) from a spout located directly in front of the mouse's mouth. The reward spout is equipped with a touch sensor allowing for accurate detection and analysis of lick rates. As mice licked the spout, during spout training day, the probability of acquiring a sucrose reward decreases. Spout training also served to habituate the mice to head fixation.

Having learned to lick the spout, mice then undergo CS+ reward conditioning. Mice receive 3 days of reward conditioning (CS+ only training session), consisting of 100 CS+ tone presentations (5 seconds duration, 70dB, 1000 or 9000 Hz), spaced out with a variable inter-trial-interval of 20-35 seconds. During these sessions mice had to lick the spout during the tone presentation to receive a sucrose droplet at tone offset. If mice did not lick the spout during the tone, they did not receive a reward at tone offset.

For CS+/CS- training, a CS- is introduced. The CS- is never rewarded. Depending on the experiment, mice are trained on CS+/CS- sessions for 7-12 days. CS+ / CS- conditioning consists of 50 random presentations of each of two distinguishable cues (5 seconds duration, 70dB, 1000 or 9000 hz), 100 tones total. A cue designated the CS+ will predict sucrose reward, while the second cue, designated CS-, will predict no reward. When the CS+ is presented, mice must lick the spout to receive a reward at tone offset. There are four outcomes from this task: hit (lick during CS+, rewarded), miss (no lick during CS+, not rewarded), false alarm (lick during CS-, not rewarded), correct rejection (no lick during CS-, not rewarded).

Modifications of behavioral protocol for 2-photon imaging

2-photon imaging required modifications to the protocol to increase the number of trials acquired. Spout training was extended to 2 days with each day consisting of one session. This was done to allow mice more habituation time to the noise generated by the 2-photon microscope. During CS+ only training sessions, 120 trials were presented, and the ITI was reduced to 10-15 seconds. During CS+/CS- training sessions, 120 trials were presented (60 CS+, 60 CS-), and the ITI was reduced to 10-15 seconds.

Modifications of chemogenetic inactivation

For chemogenetic inhibition. Mice were trained on four CS+/CS- sessions. On day 5, pre-test, all mice were injected with saline (4ul saline / gram of mouse weight). On day 6 all mice were administered CNO (3mg/kg) diluted saline (0.75 ug of CNO / ul of saline). On day 7, post-test, all mice were injected with saline (4ul saline / gram of mouse weight). Following behavioral experiments mice were perfused and brains were sliced for histological analysis to validate viral expression and injection site.

Surgery

Head Fix Surgery

For head-fixed behavior mice were implanted with a head-post. Adult (approx. P68) and adolescent (P22) mice were anesthetized with isoflurane gas anesthesia (2.0%–2.5% in 1 l/min oxygen), hair was shaved, and mice were placed in a stereotaxic apparatus. Buprenex (0.1 mg/kg, as an analgesic) was administered intraperitoneally. Tissue above the skull was cut away to reveal the skull, and lidocaine was applied. Skull was then cleaned with 0.3% hydrogen peroxide, and left to dry (no more than 2 minutes). A custom-made head post was placed on top of the skull and secured with Metabond (Parkell Inc, Brentwood, NY). After the metabond solidified, and implant was secure, isoflurane administration was stopped, and mice were allowed to wake.

Prism Implant Surgery

For 2-photon imaging, surgeries were conducted in two stages to allow for sufficient viral expression in adolescent mice. At P1-P3 neonates were placed in an isoflurane gas induction box (4% in 1 l/min oxygen). Anesthetized pups were placed in a stereotaxic apparatus where isoflurane gas was administered at a lower concentration (2.0%–2.5% in 1 l/min oxygen). Skin was cleaned, and a small sliver (approximately. 1-2 mm) was cut above the mPFC. The central sinus was located and an injector equipped with a 32 gauge beveled nanofil syringe (World Precision Instruments) preloaded with AAV1-syn-jGCaMP8f (Addgene) was lowered to the skull level. The syringe was moved to the left of the midline and lowered 1.6 mm, where a 200nL injection was delivered. The injector was raised to 1.2 mm below the skull where a second 200nL injection was delivered. The syringe was then removed and a small amount of vetbond was applied to seal the cut on the pup's skin. A second, more invasive surgery was conducted when mice reached P18 (for adolescent 2-photon imaging) or P63 (for adult 2-photon imaging). Mice were anesthetized in an isoflurane gas induction chamber (4% in 1 l/min oxygen), mouse hair was shaved, and mice were then moved to a stereotaxic apparatus where isoflurane gas was administered at a lower concentration (2.0%–2.5% in 1 l/min oxygen). Buprenex (0.1 mg/kg, as an analgesic) and Dexamethasone were co-administered intraperitoneally. Tissue above the skull was cut away to reveal the skull, and lidocaine was applied. Skull was then cleaned with 0.3% hydrogen peroxide. A ~1.2 x 1.2 mm–diameter craniotomy was drilled rostral to the left mPFC. The dura was removed from above the surface of the brain to expose the tissue. A prism (1mm X 1mm X 2.5mm; M/L, A/P, D/V) was then inserted into the craniotomy to allow imaging of the ipsilateral mPFC. A small amount of Metabond (Parkell, Brentwood, NY) was used to secure the prism in place. A headpost was then placed around the prism and a second coat of Metabond was applied to secure the headplate and the prism implant. After the metabond solidified, and implant was secure, isoflurane administration was stopped, and mice were allowed to wake. Dexamethasone was administered 24 hrs. and 48 hrs. post-surgery to decrease inflammation.

Chemogenetic Surgery

For fiber-photometry recordings of the mPFC surgeries were conducted in two stages to allow for sufficient viral expression, and secure headposts, in adolescent mice. The first surgery occurred at P16 (adolescent) and P59 - P70 (Adults). Mice were anesthetized in an isoflurane gas induction chamber (4% in 1 l/min oxygen), mouse hair was shaved, and mice were then moved to a stereotaxic apparatus where isoflurane gas was administered at a lower concentration (2.0%–2.5% in 1 l/min oxygen). Skin was cleaned, and the skin was cut along the midline. A borrow hole was drilled above mPFC (ML: ±0.32, AP: +1.5, DV: -2.1 for P16; ML: ±0.35, AP: +1.75, DV: -2.3 for adults). An injector equipped with a 32-gauge blunt nanofil

syringe (preloaded with AAV5-hSyn-DIO-hM4D(Gi)-mCherry for experimental or AAV-hSyn-DIO-mCherry for control; Addgene) into mPFC and 250nL of virus was delivered. The syringe was then removed and vetbond was applied to seal the skin incision. A second, surgery was conducted 6 days later to cement the headpost. Mice were anesthetized in an isoflurane gas induction chamber (4% in 1 l/min oxygen) and placed in a stereotaxic apparatus where isoflurane gas (2.0% - 2.5% in 1 l/min oxygen). Buprenex (0.1 mg/kg, as an analgesic) and Dexamethasone were co-administered intraperitoneally. Tissue above the skull was cut away to reveal the skull, and lidocaine was applied. Skull was then cleaned with 0.3% hydrogen peroxide. A headpost was then placed on the skull and Metabond was applied to cement the headpost. After the metabond solidified, isoflurane administration was stopped, and mice were allowed to wake.

2-photon imaging

2-photon calcium imaging was conducted using a commercial two-photon laser-scanning microscope (Olympus RS) equipped with a scanning galvanometer and a Spectra-Physics Mai Tai DeepSee laser tuned to 920nm, operating at 300-500mW. Single cells were recorded using a 10x 0.6NA objective, with 8mm working distance. To minimize the impact of photobleaching, imaging was triggered by the behavioral script. 2-photon images were acquired at 30 hz starting 5 seconds before tone onset and ending 5 seconds after tone offset (15 seconds of continuous imaging), for all 120 trial presentations. Videos were analyzed using Suite2P analysis software [38]. Cells were identified and visually inspected, neuropil and calcium neuronal trace were exported. The neuropil signal was scaled and subtracted from the cell signal (FluorescenceCell - (.7 x FluorescenceNeuropil)). Each trial of each cell was normalized by obtaining the z-scored to the first 2.5 seconds of the pretone activity. This allowed us to control for any bleaching that occurred during the session.

General Linear Model

To identify task-relevant neurons we used MATLAB's *fitglm* to identify neurons that were significant to CS+, CS-, or lick variables. GLMs were modeled with normal distributions, as linear functions (no interaction effects) and with y-intercept terms. Each individual neuron was tested on a separate GLM. If a predictor was determined significant for a given neuron, we obtained the F statistic (real F) comparing the fit of the full model to the fit of a reduced model (model without the significant predictor). We then circularly shifted (Matlab's *circshift*) the neuronal traces and re-calculated the F statistic of the fit of the full model to the fit of a reduced model over 500 iterations [39]. Neurons with a significant p-value of the predictor ($p<0.05$) and whose real F was greater than or equal to the 95th percentile of the shifted F were considered to significantly encode the task feature.

Linear decoding with SVM classifiers

To test the ability of sub-populations to decode the identity of the CS that was presented, we used a maximum-margin linear decoder (MATLAB fitcsvm). Twenty iterations were run for each neuronal subpopulation. At each iteration, data was separated into training (70%) and testing (30%) sets, with equal number of CS+ and CS- trials. The mean and SEM of the accuracy of the test set were plotted. To determine the random decoding accuracy of each subpopulation we ran 20 iterations of training sets that had shuffled labels for CS+ and CS- and tested the model on a test set with true values. Significance in decoding is determined by analyzing the significance of training with true labels compared to training with randomized labels.

General Statistical Analysis, Images, and Graphs

A two-tailed student's t-test was used to compare between two groups. When more than two groups were assessed, the appropriate ANOVA was performed as stated in the figure legends.

All ANOVA tests were followed by a multiple comparison test as detailed in the appropriate figure legend.

All ANOVA and multiple comparison tests were performed using Prism Graphpad statistical and graphing software. GLM, SVM, and correlation analysis were performed using Matlab. For all statistical analyses, statistical significance was defined as $p<0.05$. Data was graphed using Prism Graphpad and Matlab software. Schematics and pictures were created using BioRender, powerpoint, and Illustrator.

Author Contributions
GMN designed and conducted experiments and data analysis, CL provided feedback. GMN wrote the manuscript with edits provided by CL.

Acknowledgments
This work was supported by funding by the National Institutes of Health, from NIMH, NIDA, and the Hope for Depression Research Foundation to CL, and from NIMH (MH124183- GMN; MH132082- GMN) to GMN. We would like to thank Dr. Hyeyoung Shin for her help with Suite2P for analysis of 2P videos; Dr. Saba Baskoylu for feedback on experimental design, suggestions on analysis pipelines, and extensive edits on manuscript; Dr. Margaux Kenwood for feedback on decoder analysis; and Dr. Rachel Rahn for feedback on figures.

References

1. Pujara, M. & Koenigs, M. Mechanisms of reward circuit dysfunction in psychiatric illness: prefrontal-striatal interactions. *Neuroscientist* **20**, 82–95 (2014).
2. Solmi, M. *et al.* Age at onset of mental disorders worldwide: large-scale meta-analysis of 192 epidemiological studies. *Mol. Psychiatry* **27**, 281–295 (2022).
3. Hammerslag, L. R. & Gulley, J. M. Age and sex differences in reward behavior in adolescent and adult rats. *Dev. Psychobiol.* **56**, 611–621 (2014).
4. Marshall, A. T., Liu, A. T., Murphy, N. P., Maidment, N. T. & Ostlund, S. B. Sex-specific enhancement of palatability-driven feeding in adolescent rats. *PLoS One* **12**, e0180907 (2017).
5. Friemel, C. M., Spanagel, R. & Schneider, M. Reward sensitivity for a palatable food reward peaks during pubertal developmental in rats. *Front. Behav. Neurosci.* **4**, (2010).
6. Whelan, R. *et al.* Adolescent impulsivity phenotypes characterized by distinct brain networks. *Nat. Neurosci.* **15**, 920–925 (2012).
7. Romer, D. Adolescent risk taking, impulsivity, and brain development: implications for prevention. *Dev. Psychobiol.* **52**, 263–276 (2010).
8. Sasamori, H., Ohmura, Y., Kubo, T., Yoshida, T. & Yoshioka, M. Assessment of impulsivity in adolescent mice: A new training procedure for a 3-choice serial reaction time task. *Behav. Brain Res.* **343**, 61–70 (2018).
9. Moorman, D. E. & Aston-Jones, G. Prefrontal neurons encode context-based response execution and inhibition in reward seeking and extinction. *Proc. Natl. Acad. Sci. U. S. A.* **112**, 9472–9477 (2015).
10. Sparta, D. R. *et al.* Activation of prefrontal cortical parvalbumin interneurons facilitates extinction of reward-seeking behavior. *J. Neurosci.* **34**, 3699–3705 (2014).
11. Otis, J. M. *et al.* Prefrontal cortex output circuits guide reward seeking through divergent cue encoding. *Nature* **543**, 103–107 (2017).
12. Nakayama, H., Ibañez-Tallon, I. & Heintz, N. Cell-Type-Specific Contributions of Medial Prefrontal Neurons to Flexible Behaviors. *J. Neurosci.* **38**, 4490–4504 (2018).

13. Caballero, J. P., Scarpa, G. B., Remage-Healey, L. & Moorman, D. E. Differential Effects of Dorsal and Ventral Medial Prefrontal Cortex Inactivation during Natural Reward Seeking, Extinction, and Cue-Induced Reinstatement. *eNeuro* **6**, (2019).
14. Nett, K. E. & LaLumiere, R. T. Infralimbic cortex functioning across motivated behaviors: Can the differences be reconciled? *Neurosci. Biobehav. Rev.* **131**, 704–721 (2021).
15. Burgos-Robles, A., Bravo-Rivera, H. & Quirk, G. J. Prelimbic and infralimbic neurons signal distinct aspects of appetitive instrumental behavior. *PLoS One* **8**, e57575 (2013).
16. Riaz, S. *et al.* Prelimbic and infralimbic cortical inactivations attenuate contextually driven discriminative responding for reward. *Sci. Rep.* **9**, 3982 (2019).
17. Huttenlocher, P. R. Synaptic density in human frontal cortex - developmental changes and effects of aging. *Brain Res.* **163**, 195–205 (1979).
18. Petanjek, Z. *et al.* Extraordinary neoteny of synaptic spines in the human prefrontal cortex. *Proceedings of the National Academy of Sciences* vol. 108 13281–13286 Preprint at https://doi.org/10.1073/pnas.1105108108 (2011).
19. Caballero, A., Flores-Barrera, E., Cass, D. K. & Tseng, K. Y. Differential regulation of parvalbumin and calretinin interneurons in the prefrontal cortex during adolescence. *Brain Struct. Funct.* **219**, 395–406 (2014).
20. Du, X. *et al.* Prefrontal cortical parvalbumin and somatostatin expression and cell density increase during adolescence and are modified by BDNF and sex. *Mol. Cell. Neurosci.* **88**, 177–188 (2018).
21. Spellman, T., Svei, M., Kaminsky, J., Manzano-Nieves, G. & Liston, C. Prefrontal deep projection neurons enable cognitive flexibility via persistent feedback monitoring. *Cell* **184**, 2750–2766.e17 (2021).
22. Thapar, A. & Riglin, L. The importance of a developmental perspective in Psychiatry: what do recent genetic-epidemiological findings show? *Mol. Psychiatry* **25**, 1631–1639 (2020).
23. Meyer, H. C. & Lee, F. S. Translating Developmental Neuroscience to Understand Risk for Psychiatric Disorders. *Am. J. Psychiatry* **176**, 179–185 (2019).
24. Kondo, M. & Matsuzaki, M. Neuronal representations of reward-predicting cues and outcome history with movement in the frontal cortex. *Cell Rep.* **34**, 108704 (2021).
25. Klune, C. B., Jin, B. & DeNardo, L. A. Linking mPFC circuit maturation to the developmental regulation of emotional memory and cognitive flexibility. *Elife* **10**, (2021).
26. Kolb, B. *et al.* Experience and the developing prefrontal cortex. *Proc. Natl. Acad. Sci. U. S. A.* **109 Suppl 2**, 17186–17193 (2012).
27. Zimmermann, K. S., Richardson, R. & Baker, K. D. Maturational Changes in Prefrontal and Amygdala Circuits in Adolescence: Implications for Understanding Fear Inhibition during a Vulnerable Period of Development. *Brain Sci* **9**, (2019).
28. Courtin, J. *et al.* Prefrontal parvalbumin interneurons shape neuronal activity to drive fear expression. *Nature* **505**, 92–96 (2014).
29. Zhang, C. *et al.* Dynamics of a disinhibitory prefrontal microcircuit in controlling social competition. *Neuron* **110**, 516–531.e6 (2022).
30. Caballero, A. & Tseng, K. Y. GABAergic Function as a Limiting Factor for Prefrontal Maturation during Adolescence. *Trends Neurosci.* **39**, 441–448 (2016).
31. Cunningham, M. G., Bhattacharyya, S. & Benes, F. M. Increasing Interaction of amygdalar afferents with GABAergic interneurons between birth and adulthood. *Cereb. Cortex* **18**, 1529–1535 (2008).
32. Manzano Nieves, G., Bravo, M., Baskoylu, S. & Bath, K. G. Early life adversity decreases pre-adolescent fear expression by accelerating amygdala PV cell development. *Elife* **9**, (2020).
33. Willing, J., Cortes, L. R., Brodsky, J. M., Kim, T. & Juraska, J. M. Innervation of the medial prefrontal cortex by tyrosine hydroxylase immunoreactive fibers during adolescence in male and female rats. *Dev. Psychobiol.* **59**, 583–589 (2017).

34. Walker, D. M. *et al.* Adolescence and Reward: Making Sense of Neural and Behavioral Changes Amid the Chaos. *J. Neurosci.* **37**, 10855–10866 (2017).
35. Reynolds, L. M. *et al.* DCC Receptors Drive Prefrontal Cortex Maturation by Determining Dopamine Axon Targeting in Adolescence. *Biol. Psychiatry* **83**, 181–192 (2018).
36. Taniguchi, H. *et al.* A resource of Cre driver lines for genetic targeting of GABAergic neurons in cerebral cortex. *Neuron* **71**, 995–1013 (2011).
37. Madisen, L. *et al.* A robust and high-throughput Cre reporting and characterization system for the whole mouse brain. *Nat. Neurosci.* **13**, 133–140 (2010).
38. Pachitariu, M. *et al.* Suite2p: beyond 10,000 neurons with standard two-photon microscopy. *bioRxiv* 061507 (2017) doi:10.1101/061507.
39. Cox, J. *et al.* A neural substrate of sex-dependent modulation of motivation. *Nat. Neurosci.* **26**, 274–284 (2023).